Dynamical effects and conductance asymmetry in metal-insulator-metal systems with different electrodes

Tokić, B.; Šestović, D.; Marušić, Leonardo; Šunjić, Marijan

Source / Izvornik: **Physical review B: Condensed matter and materials physics, 1999, 60, 8368 - 8372**

Journal article, Published version
Rad u časopisu, Objavljena verzija rada (izdavačev PDF)

https://doi.org/10.1103/PhysRevB.60.8368

Permanent link / Trajna poveznica: https://urn.nsk.hr/urn:nbn:hr:217:932673

Dynamical effects and conductance asymmetry in metal-insulator-metal systems with different electrodes

B. Tokić, D. Šestović, L. Marušić, and M. Šunjić
Department of Physics, University of Zagreb, 10001 Zagreb, Croatia
(Received 26 February 1999)

We investigated the electron tunneling process in a planar system consisting of two semi-infinite metal electrodes of different dielectric properties separated by a narrow vacuum gap. This system can be viewed as a model of a metal-insulator-metal structure, or even as a very rough model of scanning tunneling microscopy. We used a local limit of a self-consistent dynamic calculation to evaluate effective tunneling barriers, and discussed the influence of different screening properties of the metallic electrodes on these barriers as well as on the conductance. We found that the barriers are significantly additionally lowered due to the difference in the charge fluctuation frequencies of the electrodes, and that the conductance minimum in such systems is shifted to a nonzero value. We compared our results with some measurements of *I-V* characteristics and work functions and found that our calculations contribute to the understanding of the observed conductance asymmetry. [S0163-1829(99)06735-1]

I. INTRODUCTION

The quantum phenomenon of electron tunneling is an intrinsic mechanism in many techniques and systems, where we can mention, e.g., scanning tunneling microscopy (STM) or superlattices and nanostructures. One of the most challenging questions is the calculation of electron screening in the vicinity of the electrode surfaces. The influence of dynamical screening on electron tunneling, and therefore on the conductance in tunneling junctions, was first observed in STM experiments.[1] In the interpretation of their data they used a phenomenological model for the image potential. There are, however, some other experiments that provide clear evidence of the importance of the dynamical effects, such as those performed on the semiconductor heterojunctions,[2–5] which indicate experimental parameters for which such effects become important. Also, some recent STM measurements[6,7] give information on the influence of the localized (spatially confined in the vicinity of the tip) surface-plasmon modes on the tunneling current.

Therefore there is a need for an accurate description of the image potential which will take into account the dynamical nature of the interaction, and especially the fact that the electrodes in the described systems are often made of different materials. As is well known, the classical image potential diverges near metallic surfaces,[8] and the density-functional theory (DFT) within the local-density approximation (LDA) gives an incorrect limit far away from the surface.[9] More accurate calculations of the image potential consisting of the diagrammatic corrections to the LDA result[10–13] were performed only for a single surface, while for systems consisting of two surfaces, parametrized classical barriers are usually used.[1,14] ,

In this paper we follow the approach by Jonson,[15] generalized to metal-insulator-metal (MIM) model.[16] Dynamical effects are described in terms of tunneling electron interaction with the surface plasmons (SP) which results in nonlocal electron self-energy and effective image potential. To solve this problem completely, numerical calculations should be used, but valuable insight could be gained if the theory is simplified using a local semiclassical approximation. In that case, effective barriers can even be calculated analytically if there is no external voltage applied. As shown in Refs. 16–18 even in this approximation the effective barrier ''rounds'' the edges of the static rectangular barrier, while in the presence of a finite electric field along the barrier, dynamical effects modify the transmission coefficient and barrier conductance, which has been shown by use of the path-integral method[19] or the matrix method.[20] However, the fully self-consistent dynamical effective potential, calculated from the nonlocal self-energy, differs from the one obtained in the local approximation,[21,22] especially for narrow barriers (~ 10 Å) which are becoming more and more technologically important.

Later we shall see that our results can contribute to the explanation of some features of electron tunneling, and thus help in better modeling of systems like STM,[23–26] especially as we know that theoretical results on STM resolution are behind experimental achievements.

The purpose of this paper is to analyze variations of effective barriers in MIM systems with different metals (or differently doped semiconductors). We also want to calculate the current density $j(V)$ and the conductance dj/dV in these structures, and show the influence of electron-SP coupling on the position of the barrier conductance minimum. This effect is well known in the literature[27] but it was always attributed solely to the difference of the work functions of metal electrodes. We show here that even when there is no difference in the work functions, the difference in electron screening by metallic electrodes still causes the displacement of conduction minima in conductance/voltage graphs. As was shown in Refs. 18 and 28 the difference in dielectric properties of metallic electrodes leads to asymmetries in the screening of the tunneling electron, which finally causes asymmetric tunneling characteristics. Conductance/voltage graphs shown in these papers are clearly asymmetrical indicating that their minima are displaced to a finite voltage. However, these

calculations[18,28] were not sufficiently accurate to enable quantitative determination of the minima positions. Using a more accurate quantum-mechanical description of the tunneling electron we show here how the effective tunneling barriers are affected with these effects, and numerically determine the conductance minima displacements.

II. FORMULATION OF THE PROBLEM

We investigate the system consisting of two semi-infinite metals with surfaces parallel to the $\boldsymbol{\rho}=(x,y)$ plane, separated by an insulator of width d and the electrons tunneling in the z direction. The image potential for tunneling electrons is defined in terms of the nonlocal energy-dependent self-energy evaluated in the self-consistent GW approximation[29] (i.e., neglecting the vertex corrections in the electron coupling to the charge fluctuations). As long as an electron is in the barrier region, far away from the interface, contributions from interaction with bulk plasmons and electron-hole pairs are negligible, as well as the retardation effects. Therefore we only have to account for interaction with SP modes in the long-wavelength limit. This approach is reasonable if the barrier width is large enough, so that regions close to interfaces, in which our approximation is not valid, are relatively small. For a typical value of the metal work function, $\phi \approx 5.7$ eV, the characteristic value of the wave-function decay length for the planar interface is $\sqrt{(2m/\hbar^2)\,\phi}\approx 0.8$ Å. We consider barriers 5–15-Å wide, which is large enough to satisfy the approximation and small enough to be relevant for, e.g., STM experiments.

For planar interfaces, because of parallel ($\boldsymbol{\rho}$) translational invariance, the wave function and energy can be written as

$$\psi(\mathbf{r})\sim \exp(i\mathbf{k}_\parallel\boldsymbol{\rho})\,\phi_{\mathbf{k}_\parallel}(z), \quad E=\frac{\hbar^2 k_\parallel^2}{2m^*}+E_\perp . \tag{1}$$

$\mathbf{k}_\parallel$ is the parallel electron momentum, energy $E_\perp$ is associated with electron motion perpendicular to the surface, and m^* is the effective electron mass.

The total effective potential is[21,22]

$$\tilde{V}_{\mathbf{k}_\parallel}(z,E)=V_0(z)+W_{\mathbf{k}_\parallel}(z,E), \tag{2}$$

where $V_0(z)$ is a trapezoidal barrier representing the band offset between the metal and insulator and the external voltage, and $W_{\mathbf{k}_\parallel}(z,E)$ is the induced potential inside the insulator due to the coupling with SP modes,

$$W_{\mathbf{k}_\parallel}(z,E)=\int dz'\,\Sigma_{\mathbf{k}_\parallel}(z,z',E)\,\frac{\phi_{\mathbf{k}_\parallel}(z')}{\phi_{\mathbf{k}_\parallel}(z)}. \tag{3}$$

A potential defined in such a way clearly contains nonlocal effects, but it enables us to formulate our problem by means of a local equation

$$\left[-\frac{\hbar^2}{2m^*}\frac{d^2}{dz^2}+\tilde{V}_{\mathbf{k}_\parallel}(z,E)-E_\perp\right]\phi_{\mathbf{k}_\parallel}(z)=0. \tag{4}$$

Self-energy $\Sigma_{\mathbf{k}_\parallel}$ is calculated in a self-consistent GW approximation[29]

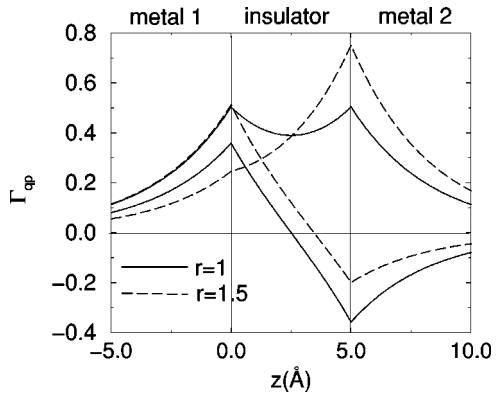

FIG. 1. Matrix elements of the electron–surface-plasmon coupling. For $r=1$ (full lines) we have standard even ($p=+$) and odd ($p=-$) modes, while for $r=1.5$ (dashed lines), there is an *in phase* ($p=+$) mode, mainly localized near the right surface, and a *counterphase* ($p=-$) mode, mainly localized near the left surface.

$$\Sigma_{\mathbf{k}_\parallel}(z,z',E)=-i\int d\mathbf{q}\,d\omega\,\mathcal{G}_{\mathbf{k}_\parallel-\mathbf{q}}(z,z',E-\hbar\omega)\times W_{\mathbf{q}}(z,z',\hbar\omega). \tag{5}$$

If we evaluate the nonlocal potential $W_{\mathbf{q}}$ in the surface-plasmon-pole approximation and integrate with respect to ω, the self-energy (5) becomes

$$\Sigma_{\mathbf{k}_\parallel}(z,z',E)=\sum_p\int d\mathbf{q}\,\Gamma_p^*(\mathbf{q},z)\times\mathcal{G}_{\mathbf{k}_\parallel-\mathbf{q}}(z,z',E-\hbar\omega_{qp})\Gamma_p(\mathbf{q},z') \tag{6}$$

where Γ's are the matrix elements of the electron-SP interaction (Fig. 1), and ω_{qp}'s are the SP mode frequencies for wave vector $\mathbf{q}$ and ''parity'' p. For $r=1$ p is a parity in the usual sense, i.e., the $p=+/-$ mode is even/odd with respect to the center of the barrier. For $r\neq 1$ none of the modes is strictly even or odd because the amplitudes on two surfaces are different, but for the $p=+$ mode oscillations on both surfaces are still in phase, while for the $p=-$ mode they are in counterphase.[18] The dispersion relation is now

$$\omega_{qp}=\frac{\omega_{p1}}{2}\sqrt{1+r^2+p\sqrt{1+r^4-r^2(2-4e^{2qd})}}, \quad r=\frac{\omega_{p2}}{\omega_{p1}}, \tag{7}$$

where ω_{p_1} (ω_{p_2}) are bulk-plasmon frequencies in the left (right) metal electrode.

The propagator $\mathcal{G}_{\mathbf{k}_\parallel-\mathbf{q}}$ is the solution of the equation

$$\left[-\frac{\hbar^2}{2m^*}\frac{d^2}{dz^2}+\tilde{V}_{\mathbf{k}_\parallel}(z,E)-E'_\perp\right]\mathcal{G}_{\mathbf{k}_\parallel-\mathbf{q}}(z)=-\delta(z-z'), \tag{8}$$

where the ''perpendicular'' energy $E'_\perp$ in the intermediate state should be evaluated from the energy conservation law

$$E=\hbar\omega_{qp}+\frac{\hbar^2(\mathbf{k}_\parallel-\mathbf{q})^2}{2m^*}+E'_\perp . \tag{9}$$

It can be shown,[30] that the solution of Eq. (8) is given by

$$\mathcal{G}_{\mathbf{k}_\parallel-\mathbf{q}}(z,z',E-\hbar\omega_i)=-\frac{2m^*}{\hbar}\frac{\phi^L_{\mathbf{k}_\parallel-\mathbf{q}}(z^>)\phi^R_{\mathbf{k}_\parallel-\mathbf{q}}(z^<)}{W(E)}, \tag{10}$$

where $\phi^{L,R}$ are solutions of Eq. (4) (with $E'_\perp$ instead of $E_\perp$), propagating from left and right, respectively, and W is their Wronskian.

We shall calculate our results in a local limit of the described nonlocal dynamical screening theory, which is equivalent to the assumption that emission and absorption of a surface plasmon by an electron occur at the same place. The validity of the approximation is discussed in Refs. 17 and 21, and it is shown that it can be used in the same cases in which the WKB approximation is valid, i.e., when the electron energy is lower than the barrier height. The local approximation requires much less numerical effort than the full dynamical calculation because one does not have to calculate the electron wave functions. For the same reason, it is suitable for generalization in curved geometries.

In the local approximation, the Green function is

$$\lim_{\kappa\to\infty}\mathcal{G}_{\mathbf{k}-\mathbf{q}}\left(z,z',\frac{\hbar^2\kappa^2}{2m}\right)=-\frac{2m}{\hbar^2\kappa^2}\delta(z-z'),$$

$$\kappa(z)=\sqrt{\frac{2m}{\hbar^2}(\tilde{V}(z)-E'_\perp)}. \tag{11}$$

Thus we have to solve an integral equation for the effective potential

$$W_{\mathbf{k}_\parallel}(z,E)=-\sum_p\int d\mathbf{q}\frac{|\Gamma_p(\mathbf{q},z)|^2}{\tilde{V}(z)-E'_\perp}. \tag{12}$$

In the first step we assume that $\tilde{V}(z)=V_0(z)$, where V_0 is linear in z, and then iterate until self-consistency is achieved.

Following Ref. 31, for the calculation of the current density we use

$$j(V)=\frac{2e\rho_\parallel}{h}\left[eV\int_0^{E_F-eV}D(E_z,V)dE_z+\int_{E_F-eV}^{E_F}D(E_z,V)(E_F-E_z)dE_z\right], \tag{13}$$

where $D(E_z,V)$ is a transmission probability for the effective barrier in WKB approximation.

III. RESULTS AND DISCUSSION

Our MIM model with different metallic electrodes can be viewed as a planar model of an electronic device with differently doped semiconductors, or even as a starting point of a model for STM which consists of two planar surfaces with a protrusion or an adsorbed atom (or molecule) on one of them. First we want to discuss the shape of the calculated effective barriers. We find that dynamical effects lower the barrier even more than in the case of the same metals.[21,22] The lowering is stronger if the difference between two bulk-plasmon frequencies increases, and the barrier also becomes more asymmetric. The results are shown in Fig. 2.

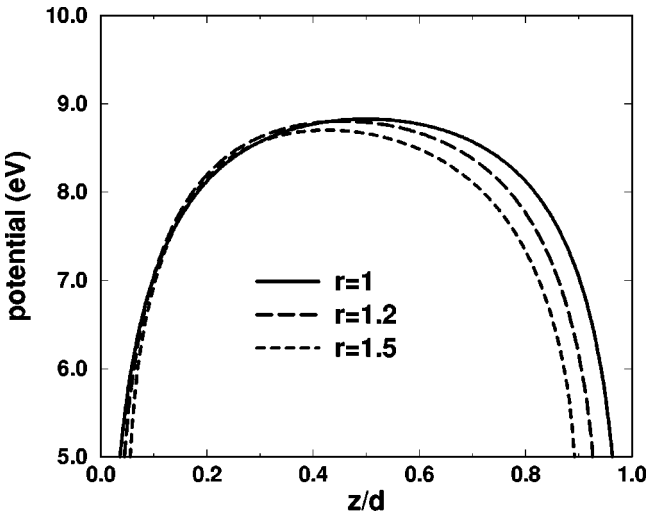

FIG. 2. Effective barriers for three different values of plasmon frequency ratio r (indicated in the figure). Static barrier width is $d=5$ Å and height is $V_0=10$ eV. Plasmon frequency ω_{p_1} is 10 eV (close to the value for tungsten) and $\omega_{p_2}=r\omega_{p_1}$.

In order to quantify these changes we calculated the maximum height (top) of effective barrier and transmission probability as functions of the plasmon frequency ratio $r=\omega_{p_1}/\omega_{p_2}$ (Fig. 3). First, we notice an abrupt change in the maximum height of the barrier when $r\neq1$, as the symmetry of the problem is broken. The shape of the kinks on both curves is probably due to the relatively small number of calculated points, but the peak at $r=1$ is real; it results from the resonance between two bulk-plasmon frequencies when electrodes have the same dielectric properties.

The screening of a charge particle placed near a metal surface results from coupling to the charge-density fluctuations in the metal which is usually intuitively described in terms of an ''image'' created in the metal and having an opposite charge with respect to that of the original particle. For a charge between two surfaces, not just the image of the original particle is created, but also an image of the image at the opposite surface, with the charge opposite to that of the first image, etc., resulting in a series of higher-order images. For metals with the same dielectric properties—same plasma

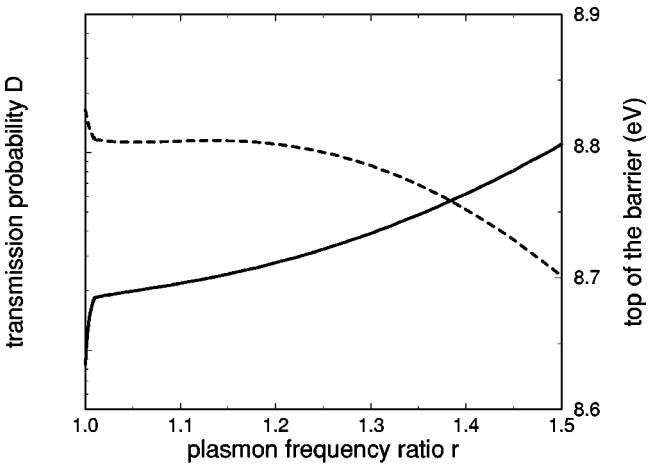

FIG. 3. Top of the effective barrier (dashed line) and transmission probability D (full line) as functions of the plasmon frequency ratio r for external bias $V=0$.

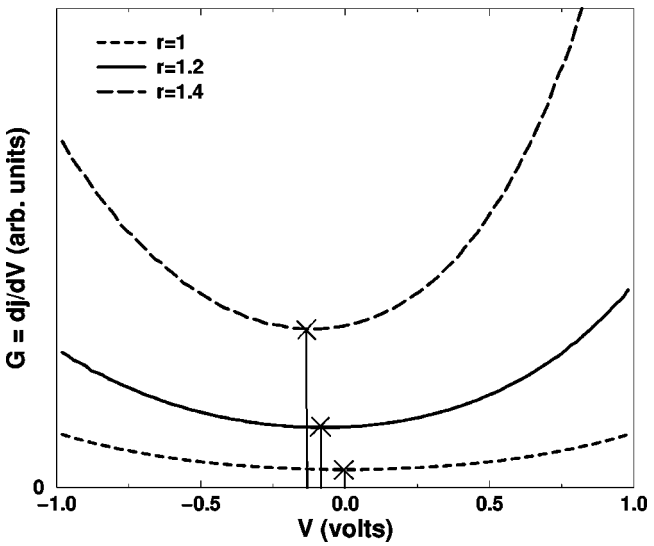

FIG. 4. Conductance G versus external bias V (in volts) for static barrier width $d=5$ Å and three different values of r. For $r=1$ the curve is symmetrical with the minimum for $V=0$, while for $r\neq 1$ curves are asymmetrical and the minima are displaced to some finite voltage (indicated by crosses).

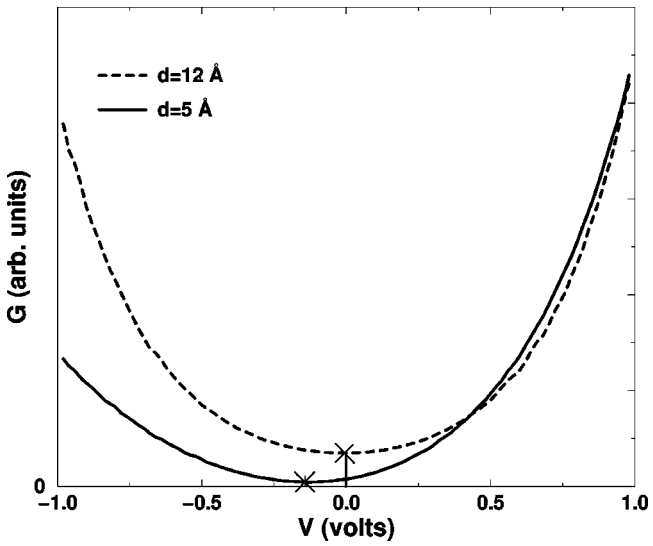

FIG. 5. Same as Fig. 4, but for a fixed plasmon frequency ratio ($r=1.5$) and for two different static barrier widths (indicated in the figure).

frequencies ($r=1$), each higher-order image reduces the screening effect of the lower-order image. If, however, the electrodes do not have the same plasma frequencies ($r\neq 1$), this resonance is broken in the dynamical calculation, and the images of higher order are much weaker, i.e., the screening is stronger. In the case (large r) when charge fluctuations in two electrodes are effectively decoupled the total screening is simply the sum of the contributions from two noninteracting surfaces.

Second, we notice that for typical metallic plasmon frequencies, the height of the barrier does not decrease monotonously as r increases. For $1.06<r<1.14$ the barrier is slightly increasing (or at least constant, but definitely not decreasing). However, as can be seen in Fig. 2, even if the barrier maximum height is not reduced, its width is, so the transmission probability is a monotonously increasing function of r.

In the case of different metals, the transmission probability $D(V)$, the current density $j(V)$ and the conductance $G(V)$ are asymmetric with respect to the bias polarity. Throughout this paper we assumed that there is no contact potential, so the asymmetry of the conductance obviously results from the difference in the plasma frequencies of the electrodes.

The conductance $G(V)$, calculated for the system of tungsten and gold electrodes separated by a vacuum gap, is shown in Figs. 4 and 5. It is roughly of parabolic shape, but clearly asymmetric. Moreover, the conductance minima are shifted to some nonzero values V_{off} (denoted with crosses). The absolute value of the offset $|V_{off}|$ increases with r or, when r is fixed, as the distance between electrodes d decreases. In the literature, the origin of the nonzero offset was explained as due either to the nonzero contact potential (Ref. 27 and the references within) or the nonzero surface curvature.[18] Here we have calculated nonzero offset in a planar model as a consequence of a solely dynamical effect in a system with different electrodes. There is a limited experimental evidence of this offset because it has a rather small value, but interesting measurements can be found in Refs. 32 and 33. The authors were measuring *I-V* characteristics in a STM experiment with differently doped Si samples. For highly doped samples they found that the spectra were shifted. The shift was attributed to the band bending on a Si surface. However, Allen and Gobeli[34] found that the work function for a Si surface is changed about 0.1 eV (2% of the work function) when the doping is increased from intrinsic Si to the values of doping that were used in Refs. 32 and 33. On the other hand, plasmon frequencies in these two samples differ over several orders of magnitude. Although we cannot quantitatively predict the magnitude of the offset in the experimental setting described in Refs. 32 and 33, we assume that the measured offset is at least in part, if not mainly, due to the difference in plasma frequencies of differently doped samples. Also, it is obvious that the shape of the experimental conductance/voltage curves (Fig. 5 in Ref. 33) is qualitatively the same as the shape of our calculated curves (Figs. 4 and 5).

IV. CONCLUSION

In this paper we have shown the importance of dynamical effects in the calculation of tunneling current density, e.g., in STM and other systems that can be approximated with a metal-insulator-metal model. The introduction of different plasma frequencies brings asymmetry into an otherwise symmetrical model. The result is a shift of the conductance minima to a finite voltage. We have shown that this shift could be a consequence of dynamical effects only, regardless of a system geometry and the contact potential. In systems with semiconducting constituents the shift was previously explained as the consequence of band bending at the semiconductor surface. However, we think that band bending need not always be sufficiently strong to explain such a shift

of the conductance minima, and that the tunneling electron screening by plasma fluctuations should also be taken into account.

Our main concern was to find a theoretical treatment of the process able to connect the classical description and the LDA-DFT approach when an electron is positioned several Å from metal electrodes, i.e., in the region where both theories fail to explain the image potential. The potential derived in this paper meets this requirement and provides a simple expression that can be used, e.g., in the calculation of STM, for small separations of tip and sample, and similar experiments.

[1] G. Binnig, N. Garcia, H. Rohrer, J. M. Soler, and F. Flores, Phys. Rev. B **30**, 4816 (1984).

[2] P. Guéret, E. Marclay, and H. P. Meier, Appl. Phys. Lett. **53**, 1617 (1984).

[3] P. Guéret, C. Rossel, E. Marclay, and H. P. Meier, J. Appl. Phys. **66**, 278 (1989).

[4] P. Guéret, C. Rossel, W. Schlup, and H. P. Meier, J. Appl. Phys. **66**, 4312 (1989).

[5] C. Rossel, P. Guéret, and H. P. Meier, J. Appl. Phys. **67**, 900 (1990).

[6] R. Berndt, J. K. Gimzewski, and P. Johansson, Phys. Rev. Lett. **67**, 3796 (1991).

[7] R. Berndt, J. K. Gimzewski, and P. Johansson, Phys. Rev. Lett. **71**, 3493 (1993).

[8] J. D. Jackson, *Classical Electrodynamics* (Wiley, New York, 1975).

[9] N. D. Lang and W. Kohn, Phys. Rev. B **1**, 4555 (1970).

[10] A. G. Eguiluz, M. Heinrichsmeier, A. Fletzar, and W. Hanke, Phys. Rev. Lett. **68**, 1359 (1992).

[11] J. J. Deisz, A. G. Eguiluz, and W. Hanke, Phys. Rev. Lett. **71**, 2793 (1993).

[12] M. Heinrichsmeier, A. Fletzar, and W. Hanke, and A. G. Eguiluz, Phys. Rev. B **57**, 14 974 (1998).

[13] H. N. Rojas, R. W. Godby, and R. J. Needs, Phys. Rev. Lett. **74**, 1827 (1995).

[14] J. M. Pitarke, P. M. Echenique, and F. Flores, Surf. Sci. **217**, 267 (1989).

[15] M. Jonson, Solid State Commun. **33**, 743 (1980).

[16] D. B. Tran Thoai and M. Šunjić, Solid State Commun. **77**, 955 (1991).

[17] M. Šunjić and L. Marušić, Phys. Rev. B **44**, 9092 (1991).

[18] D. Šestović, L. Marušić, and M. Šunjić, Phys. Rev. B **55**, 1741 (1997).

[19] N. Klipa and M. Šunjić, Phys. Rev. B **52**, 12 408 (1995).

[20] H. Ness and A. J. Fisher, J. Phys.: Condens. Matter **10**, 3697 (1998).

[21] M. Šunjić and L. Marušić, Solid State Commun. **84**, 123 (1992).

[22] L. Marušić and M. Šunjić, Solid State Commun. **88**, 781 (1993).

[23] N. D. Lang, Phys. Rev. Lett. **55**, 230 (1985).

[24] N. D. Lang, Phys. Rev. Lett. **56**, 1164 (1986).

[25] G. Doyen, D. Drakova, J. V. Barth, R. Schuster, T. Gritsch, R. J. Behm, and G. Ertl, Phys. Rev. B **48**, 1738 (1993).

[26] Th. Laloyaux, I. Derycke, J.-P. Vigneron, Ph. Lambin, and A. A. Lucas, Phys. Rev. B **47**, 7508 (1993).

[27] E. L. Wolf, *Principles of Electron Tunneling Spectroscopy* (Oxford University Press, Oxford, 1989).

[28] D. Šestović and M. Šunjić, Solid State Commun. **98**, 375 (1996).

[29] J. J. Quinn and R. A. Ferrel, Phys. Rev. **112**, 812 (1958); L. Hedin and S. Lundqvist, *Solid State Physics* edited by H. Ehrenreich, F. Seitz, and D. Turnbull (Academic, New York, 1969), Vol. 23, p. 1.

[30] P. M. Morse and H. Fesbach, *Methods of Theoretical Physics* (McGraw-Hill, New York, 1953).

[31] C. B. Duke, *Tunneling in Solids*, edited by F. Seitz and D. Turnbull, Solid State Physics Suppl. 10 (Academic, New York, 1969).

[32] J. A. Stroscio, R. M. Feenstra, and A. P. Fein, Phys. Rev. Lett. **57**, 2579 (1986).

[33] J. A. Stroscio, R. M. Feenstra, and A. P. Fein, Surf. Sci. **181**, 295 (1987).

[34] F. G. Allen and G. W. Gobeli, Phys. Rev. **127**, 150 (1962).